IAC-14-C1.3.4

ATTITUDE CONTROL OF LARGE GOSSAMER SPACECRAFT USING SURFACE REFLECTIVITY MODULATION

Andreas Borggräfe
Advanced Space Concepts Laboratory, Department of Mechanical and Aerospace Engineering, University of Strathclyde, Glasgow, Scotland G1 1XJ, United Kingdom,
E-Mail: andreas.borggraefe@strath.ac.uk

Jeannette Heiligers
Advanced Space Concepts Laboratory, Department of Mechanical and Aerospace Engineering, University of Strathclyde, Glasgow, Scotland G1 1XJ, United Kingdom,
E-Mail: jeannette.heiligers@strath.ac.uk

Matteo Ceriotti
School of Engineering, University of Glasgow, Glasgow, Scotland G12 8QQ, United Kingdom,
E-Mail: matteo.ceriotti@glasgow.ac.uk

Colin R. McInnes
Advanced Space Concepts Laboratory, Department of Mechanical and Aerospace Engineering, University of Strathclyde, Glasgow, Scotland G1 1XJ, United Kingdom,
E-Mail: colin.mcinnes@strath.ac.uk

Gossamer spacecraft are ultra-lightweight structures which deploy large, thin reflective membranes. Since the on-board attitude control systems need to be high-performance, reliable and importantly lightweight, this work investigates the use of thin-film reflectivity control devices across the membrane surface for attitude control. These coating elements can modify their surface reflectivity, which modulates the solar radiation pressure acting on the surface. Consequently, the total body force and torque can be controlled 'optically' without using additional mechanical systems or thrusters. The membrane is modelled using discrete reflectivity cells (as in a dot matrix) across the surface. The elements can maintain two states: either high (power on) or low reflectivity (power off). The aim is towards finding the optimal reflectivity pattern in terms of number and combination of active cells to create a required control torque. The control problem is solved using a quaternion feedback scheme, under consideration that the system is under-actuated, since through the concept of surface reflectivity modulation presented here, torques can be created in the membrane plane only. The optical actuator is applied successfully to perform a basic spacecraft manoeuvre from an initial arbitrary attitude state towards Sun-pointing on a Sun-centred orbit.

I. INTRODUCTION

Given their capabilities, developing large and ultra-lightweight space membrane reflectors is already within the technology roadmaps of leading space agencies such as NASA, ESA and JAXA. Gossamer spacecraft essentially consist of a highly-reflective thin film, folded into a packed configuration during launch. Once delivered into orbit, the membrane is deployed from a supporting structure and forms a large reflective surface. This type of spacecraft achieves very low mass and small stowage volume and thus enables various space-based applications such as large communication antennae, solar energy collectors and solar sails. The ability to control such a large membrane in space is essential for its successful operation. In order to increase the flexibility of modulating the spacecraft body torques, and to decrease the total mass of the spacecraft, the attitude dynamics of a rigid, flat reflective membrane with a variable surface reflectivity distribution is investigated. The reflectivity can in principle be

modified using so called reflectivity control devices (RCDs), which consist of an electro-active material that changes its surface reflectivity according to an applied electric potential.[1] Electro-chromic coatings have already been employed successfully for attitude control on the IKAROS solar sail (Japan), in 2010[2].

The paper will demonstrate the potential of modulating the surface reflectivity for optical control of the spacecraft attitude. In section II, the model of a flat rigid membrane reflector using a number of square RCD cells across the surface will be introduced. The achievable discrete in-plane torques will be derived, as a function of number, position and activation state of the coating elements as free parameters. Through this concept, a wide range of torque vector directions in the sail-plane can be generated, while torques perpendicular to the surface are zero. Subsequently, in section III, the attitude control framework will be outlined, using a quaternion feedback controller to compute the reference torques that have to be matched by the actuating RCD matrix in order to steer the spacecraft. This has to take into account that the optical attitude controller can deliver a control torque with two components only for controlling three rotational degrees of freedom. Further, the two in-plane torque components both depend on the distribution and activation state of the RCD elements simultaneously, thus they cannot be controlled independently. In addition, also the available torque magnitude decreases with increasing pitch angle, which is the light-incidence angle between the Sun-membrane line and the surface normal. Therefore, the torque magnitudes vary with changing spacecraft attitude, and this constitutes a challenging attitude control problem. In section IV, the concept will be demonstrated for two-axis attitude control of the spacecraft on a Sun-centred orbit at 1 AU solar distance. It will be shown that through a basic manoeuvre about two axes, the sail can be brought to a Sun-pointing attitude from a chosen initial displacement and rotation state.

II. MEMBRANE SPACECRAFT MODEL WITH REFLECTIVITY CONTROL CELLS

A body-fixed Cartesian coordinate frame $\mathcal{B} := (\boldsymbol{x}, \boldsymbol{y}, \boldsymbol{z})$ is used to describe the membrane attitude, with $(\boldsymbol{x}, \boldsymbol{y})$ in the membrane plane and $\boldsymbol{z}$ in surface normal direction, as shown in figure 1. Throughout this work, the so called ecliptic reference frame $\mathcal{E} := (\boldsymbol{x}_\mathrm{E}, \boldsymbol{y}_\mathrm{E}, \boldsymbol{z}_\mathrm{E})$ is used, centred in the spacecraft CoM on a Sun-centered orbit. The $\boldsymbol{z}_\mathrm{E}$ axis is oriented towards the Sun, the $\boldsymbol{y}_\mathrm{E}$ component is always

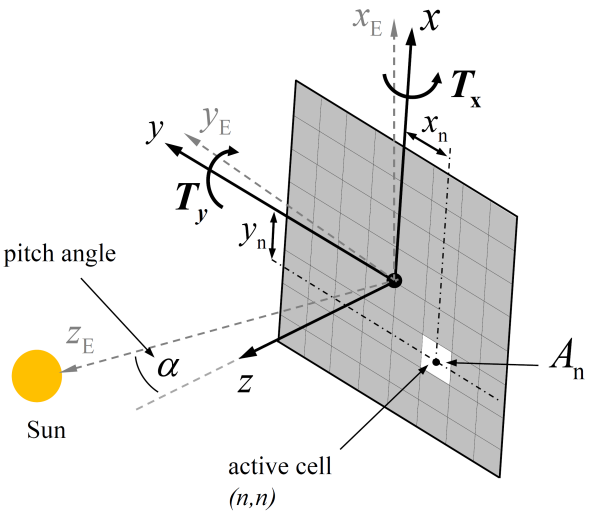

Figure 1: Square membrane reflector spacecraft with discrete number of RCD cells across the surface to modulate SRP torques acting on the structure for attitude control

in the ecliptic plane, and $\boldsymbol{x}_\mathrm{E}$ completes the right-handed coordinate system.

The membrane surface A is covered with a square matrix $M := (n, n)$ of electro-chromic coating cells (RCDs) that are restricted to operate at two discrete reflectivity states, either 'on' ($\rho_\mathrm{on} = 1$) or 'off' ($\rho_\mathrm{off} = 0$). The additional mass and thickness of the elements is neglected throughout this study. The solar radiation pressure (SRP) that is acting on each RCD element is calculated using a simplified SRP model.[3] It assumes that the active element surface is a perfectly (specular) reflecting mirror, neglecting all other forms of optical interactions between the solar photons and the surface such as scattering, absorption and thermal re-emission. Accordingly, the solar radiation pressure p_SRP is always perpendicular to the surface and can be written as

$$p_\mathrm{SRP} = p_0 \left[1 + \rho\right] \left(\frac{R_{S,0}}{R_S}\right)^2 \cos^2 \alpha \qquad (1)$$

at a radial distance R_S from the Sun and $p_0 = 4.563 \times 10^{-6} \mathrm{N/m^2}$ being the solar radiation pressure at $R_{\mathrm{S},0} = 1$ AU. The pitch angle α denotes the current angle between the Sun-spacecraft line and the membrane surface normal. In Eq. 1, $\rho_\mathrm{on} = 1$ represents the ideal mirror that experiences the maximum possible SRP load $p_\mathrm{max} = 2p_0$, while the minimum reflectivity ($\rho_\mathrm{off} = 0$) reduces the effective SRP load to $p_\mathrm{max}/2 = p_0$, since only the momentum of the incoming photons applies a force to the surface. As a consequence, the SRP induced forces can be modified directly when changing the surface reflectivity

of the RCD elements. Accordingly, each equal cell n of area $A_n = \Delta x\,\Delta y$ and distance x_n and y_n from the in-plane body axes $\boldsymbol{x}$ and $\boldsymbol{y}$, respectively, creates a torque $\boldsymbol{T}_n = (T_{\mathrm{x,n}}, T_{\mathrm{y,n}})$. However, no torque is generated in surface normal direction $\boldsymbol{z}$. Written in x and y-components, the SRP torques created by each individual element n at 1 AU solar distance are

$$T_{\mathrm{x},n} = -p_0\,[1+\rho]\cos^2\alpha\,y_n\,A_n \tag{2a}$$

$$T_{\mathrm{y},n} = \quad p_0\,[1+\rho]\cos^2\alpha\,x_n A_n \tag{2b}$$

with $\rho \in (\rho_{\mathrm{on}}, \rho_{\mathrm{off}})$. Depending on the number and activation state of distributed reflectivity elements across the surface, a wide range of total torques can be generated in the membrane plane.

The number of possible reflectivity combinations using two-state elements (on/off) follows the relation

$$C = 2^{n^2} \tag{3}$$

and thus, increases rapidly with increasing size of the square RCD element matrix M, as shown in table 1. For example, using a (6×6)-matrix, thus a

Table 1: Number of possible reflectivity control combinations C as function of square matrix size (n, n) and total element number N

n	N	C
2	4	16
3	9	512
4	16	65,536
5	25	33.554×10^6
6	36	68.719×10^9

total number of $N = 36$ elements across the surface, the number of possible combinations C is already 68.7 billion. However, every symmetric combination does not create a torque, since opposite elements cancel out. In addition, each inverted combination generates the exact counter torque about both in-plane axes, as indicated for a (3×3)-array in Fig. 2. The figure shows one subset of the total 512 combinations, in which each individual creates the same torques about the x and y-axis. Only the sign of the two torques changes, as indicated by the $(+)$ and $(-)$ sign on top of each column. For example, the two solid frames mark two symmetric combinations, one from the $(++)$ column, one from the $(--)$ column. As can be seen, middle elements only produce torque about one axis at a time. The centre-element never produces a torque. Therefore, the total number of discrete torques N_{T} that can

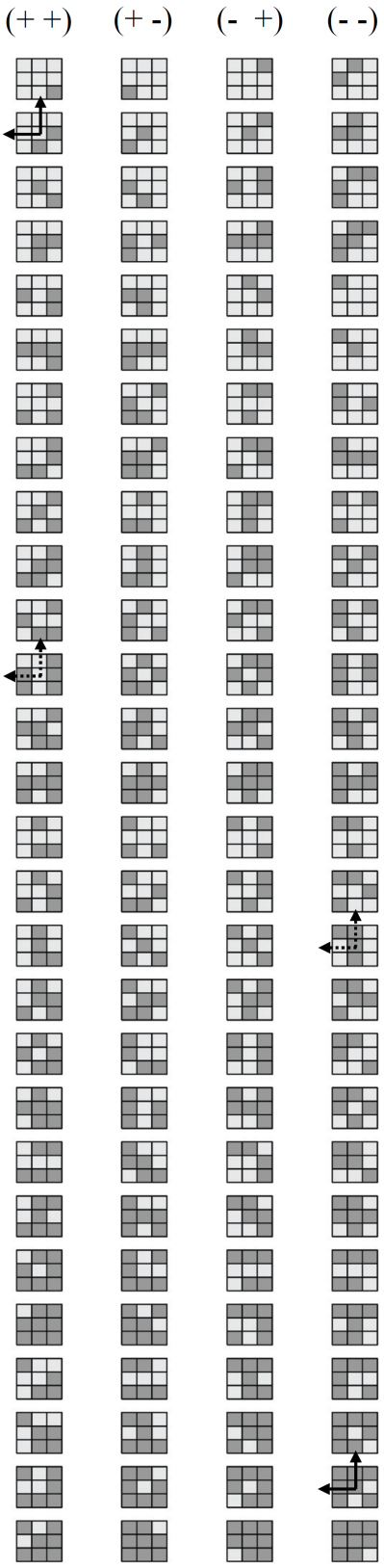

Figure 2: Largest subset of possible reflectivity combinations using (3×3)-array. Each combination generates same torque magnitude about body x and y-axis. T_{x} and T_{y} directions different in each column, as indicated with + (positive) and - (negative)

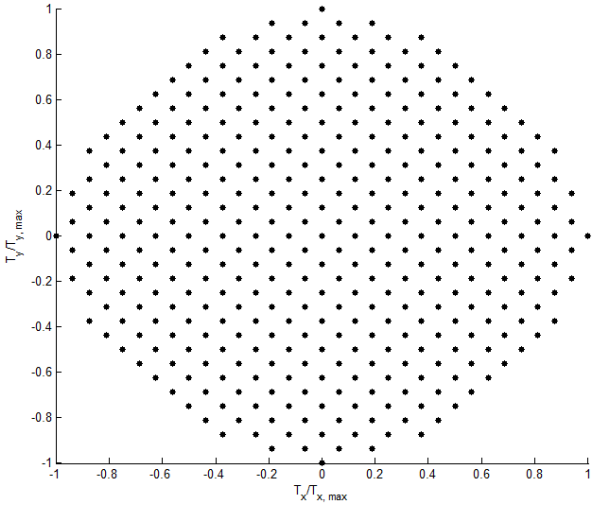

Figure 3: Non-dimensional discrete torques in x and y-components, generated by a (4×4)-array. Each entry may contain several reflectivity combinations resulting in the same torque

be generated is much smaller than C. For example, when collecting same-torque combinations using a (4×4)-array, this number is $N_{\mathrm{T}} = 376 + 1$, including zero-torque combinations. The individual torque-pairs are shown in Fig 3, normalized by the maximum possible torque about each in-plane axis, $T_{\mathrm{x,max}}$ and $T_{\mathrm{y,max}}$. The distance between two torque pairs in x and y-direction represents the minimum discrete torque increment that can be generated using a (4×4)-array. This already indicates potential challenges for membrane attitude control, in case a limited number of elements across the surface is used. The total torque that can be generated varies significantly, as can be seen in Fig 4.

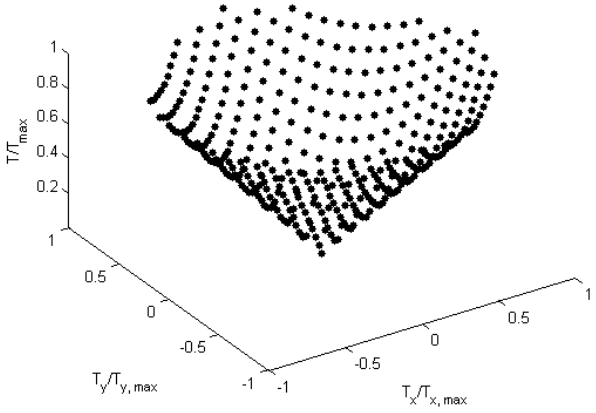

Figure 4: Non-dimensional discrete torques in x and y-components, generated by a (4×4)-array, and total magnitude of the torque

III. OPTICAL ATTITUDE CONTROL

In the following, a feedback control scheme for two-axis attitude control of the membrane spacecraft using a discrete $(n \times n)$ RCD actuation matrix on the surface is introduced. The rigid-body attitude dynamics of the spacecraft are described using Euler's Equation in quaternion notation.[4] Choosing quaternions for attitude representation is beneficial compared to other attitude descriptors such as Euler angles, since quaternions have only one redundant parameter (no singularities) and offer a lower computational effort (no trigonometric functions).[5,6] In the present analysis, it is assumed that attitude changes are not affecting the spacecraft's Sun-centred orbit, thus the orbit and attitude motion are decoupled. The governing kinematic equation of the rotational motion of a rigid body can be written as

$$\dot{\bar{q}} = \frac{1}{2}\, \bar{q} \otimes \bar{\omega} \tag{4}$$

which represents the first derivative of the attitude quaternion $\bar{q}$ due to the angular velocity $\bar{\omega} = [0, \omega_{\mathrm{x}}, \omega_{\mathrm{y}}, \omega_{\mathrm{z}}]^{\mathrm{T}}$. The upper $(\bar{})$ denotes a quaternion vector

$$\bar{q} = q_1 + \boldsymbol{q} = \cos\left(\frac{\theta}{2}\right) + \boldsymbol{a} \cdot \sin\left(\frac{\theta}{2}\right) \tag{5}$$

with the rotation angle θ about the Euler-axis of rotation $\boldsymbol{a}$, which is defined with respect to the body frame $\mathcal{B}$. The operator $\otimes$ represents the quaternion product.[5]

Furthermore, the Euler equation describes the change of angular velocity $\dot{\bar{\omega}}$ due to an external torque $\boldsymbol{T}$ about the body axes such as

$$\dot{\boldsymbol{\omega}} = \left([I]^{-1}(\boldsymbol{T} - \boldsymbol{\omega} \times [I]\boldsymbol{\omega})\right) \tag{6}$$

with $[I]$ the mass moment of inertia tensor.

The above Eqs. 4 and 6 can be solved numerically by formulating the initial value problem

$$\bar{q}(0) = \bar{q}_0, \quad \boldsymbol{\omega}(0) = \boldsymbol{\omega}_0 \tag{7}$$

and using, for example, the MATLAB$^{\mathrm{TM}}$ *ode45* routine that employs a explicit Runge-Kutta (4,5) scheme.[7] The system is controlled using a quaternion feedback scheme in Simulink$^{\mathrm{TM}}$, as shown in Fig 5. The scheme calculates the error quaternion $\bar{q}_{\mathrm{err}}$ between the desired reference attitude $\bar{q}_{\mathrm{ref}}$ and the current attitude $\bar{q}_{\mathrm{i}}$ at time t_i, by the quaternion product

$$\bar{q}_{\mathrm{err}} = \bar{q}_{\mathrm{ref}} \otimes \bar{q}_{\mathrm{i}} \tag{8}$$

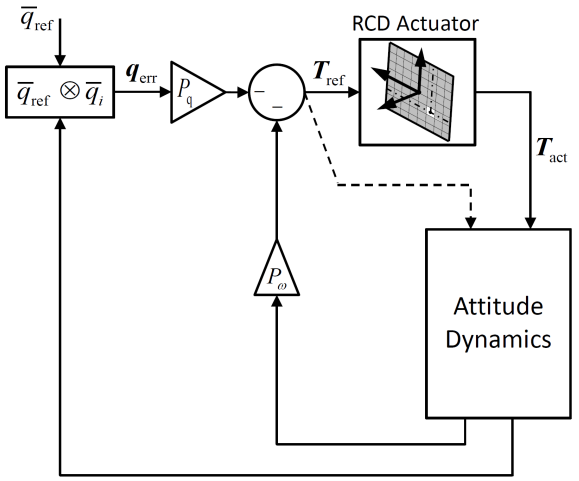

Figure 5: Quaternion feedback control scheme. Dashed line indicating reference torque $\boldsymbol{T}_{\mathrm{ref}}$ loop without RCD actuation $\boldsymbol{T}_{\mathrm{act}}$

According to Fig. 5, a non-linear P^2-controller formulation has been implemented, consisting of two loops: an inner loop using a proportional controller P_ω for the angular velocity and an outer loop proportional controller P_{q} for the tracking of the current attitude error, which can be formulated as[8]

$$\boldsymbol{T}_{\mathrm{ref}} = -P_{\mathrm{q}} \cdot \boldsymbol{q}_{\mathrm{err}} - P_\omega \cdot \boldsymbol{\omega}_{\mathrm{i}} = \begin{pmatrix} T_{\mathrm{x,ref}} \\ T_{\mathrm{y,ref}} \\ 0 \end{pmatrix} \qquad (9)$$

with $\boldsymbol{q}_{\mathrm{err}}$ the vector component of the current error quaternion, according to Eq. 5. The $T_{\mathrm{z,ref}}$ component is be neglected, since it cannot be provided by the employed RCD actuator. The values of the gains P_ω and P_{q} are defined empirically such that the output $\boldsymbol{T}_{\mathrm{ref}}$ matches the maximum torque $\boldsymbol{T}_{\mathrm{act}}$ achievable by the RCD actuator. The maximum torque is generated when one half of the surface is set to reflectivity $\rho = 1$, while $\rho = 0$ for the other half.

Before executing the control loop, the RCD actuator is initialised by calculating all possible discrete torques $(T_{\mathrm{x}}, T_{\mathrm{y}})_{\mathrm{act}}$ for the employed RCD array. The torques are stored in a lookup table, together with the respective combination number of the active element(s). For example, the set of possible torques using a (4×4) element array has been shown in Fig. 3. When the control loop is active, the controller returns the reference torque $(T_{\mathrm{x}}, T_{\mathrm{y}})_{\mathrm{ref}}$, according to Eq. 9, which is then provided to the optical RCD actuator. In here, the achievable torque from the employed $(n\times n)$ RCD-array is computed by browsing the lookup table of discrete RCD torques. In particular, the best achievable torque $(T_{\mathrm{x}}, T_{\mathrm{y}})^*_{\mathrm{act}}$ is found by scanning the lookup table for the closest match in body x and y-direction. As mentioned before, the actuator array can only generate a finite number of torques, with the torque magnitude further depending on the current surface pitch angle α towards the Sun, according to Eq. 1. Finally, $(T_{\mathrm{x}}, T_{\mathrm{y}})^*_{\mathrm{act}}$ is further used within the Euler equations to compute the new attitude. Alternatively, the feedback control loop can also be executed without the RCD actuator, thus controlling the spacecraft attitude directly using the reference torque $\boldsymbol{T}_{\mathrm{ref}}$, as through Eq. 9.

IV. SPACECRAFT ATTITUDE MANEUVER USING DISCRETE RCD ARRAY

The optical RCD actuator is now applied to control the attitude of a membrane reflector spacecraft on a Sun-centered orbit. Starting from an arbitrary initial attitude and spin rate, the final spacecraft attitude shall be towards Sun-pointing, using combined RCD torques $(T_{\mathrm{x}}, T_{\mathrm{y}})$ in the membrane surface plane. The final attitude in body z-direction is not controllable and will be neglected throughout the present analysis. A sample square membrane reflector configuration is modelled using a flat rigid Kapton[9,10] film of edge length $L = 100$ m. Including the membrane assembly mass and the payload mass, the total mass of the spacecraft is assumed to be $m = 200$ kg. Accordingly, the mass moments of inertia of the structure are $I_{\mathrm{xx}} = I_{\mathrm{yy}} = 1.67 \times 10^5$ kg m^2 and $I_{zz} = 3.34 \times 10^5$ kg m^2.

The optical controller shall perform a basic spacecraft maneuver towards Sun-pointing, thus pitch angle $\alpha_{\mathrm{final}} = 0$. Initially, the membrane surface is chosen to be tilted by the Euler angles $\theta_{\mathrm{x},0} = \theta_{\mathrm{y},0} = -40$ deg about the in-plane $\boldsymbol{x}$ and $\boldsymbol{y}$-axis. This attitude translates into an initial pitch angle displacement of $\alpha_0 = 54$ deg. Additionally, the spacecraft is rotating with an angular rate of $\omega_{\mathrm{x}} = \omega_{\mathrm{y}} = 0.1$ deg/s. First, the manoeuvre is controlled using the reference torques $\boldsymbol{T}_{\mathrm{ref}}$ from the ideal feedback controller, without the optical RCD actuation, as shown by the dashed path in Fig. 5. Secondly, a (4×4) RCD-array is used to translate the reference torques into the closest-match optical SRP torques, as achievable by the employed array. As shown in Section II, this array has $C = 65,536$ reflectivity combinations, however, the number of discrete torques that can be achieved reduces to $N_{\mathrm{T}} = 376+1$, including zero-torque. The maximum possible torque about each axis of the sample membrane are found to be $T_{\mathrm{x,max}} = T_{\mathrm{y,max}} = \pm 0.57$ Nm, which occurs when all coating elements on one half

of the surface are active.

The second control setup, using the RCD actuator array, will further be repeated including the effect of the current membrane pitch angle α on the SRP torques during the manoeuvre, as shown in Eq. 1.

The resulting reference control torques $(T_\mathrm{x}, T_\mathrm{y})_\mathrm{ref}$ for the chosen attitude manoeuvre, as computed by the controller (Eq. 9), are shown in Fig. 7. The simulation is aborted at the time t_end for which $\alpha(t)$ stays below a certain threshold $\alpha_\mathrm{lim} \leq 0.1\,\mathrm{deg}$. This is achieved at the time $t_\mathrm{end} = 3000\,\mathrm{s} = 50\,\mathrm{min}$. The simulation is repeated after activating the (4×4)-array RCD actuation. The achievable torques from the RCD actuator are now given in Fig. 8. Although the individual torque magnitudes are partly staying below the reference, Fig. 7, the RCD actuator can follow the controller's demands by returning the closest matching torques available. When including the pitch angle influence on the SRP during the manoeuvre, according to Fig. 9, the actuated torques $(T_\mathrm{x}, T_\mathrm{y})_\mathrm{act}$ are modulated to lower values, in particular for high $\alpha(t)$. According to Fig. 6, the pitch angle is highest at the start of the simulation and during the time interval $[700, 1500]$, when the membrane is overshooting the target Sun-pointing attitude. The overshooting is higher in case of the RCD actuation (dashed line in Fig. 6), due to the limited capacity of the RCD-array to provide the required control torques. The pitch angle reaches the required α_lim condition in approximately twice the simulation time, which is likely to be due to the minimum threshold of discrete torque that can be generated by the employed RCD-array.

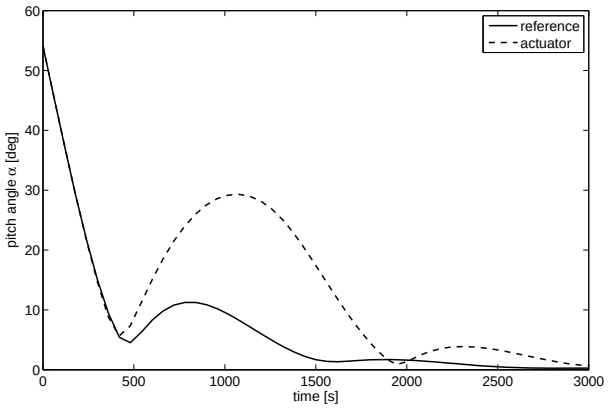

Figure 6: Membrane surface pitch angle α time-history using reference torque control (solid line) and using RCD actuator control, considering SRP variation with α (dashed line)

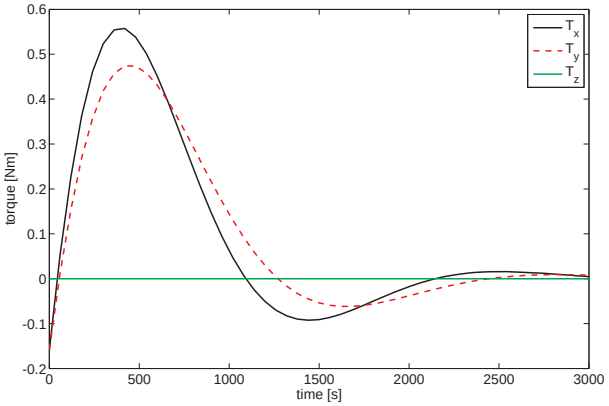

Figure 7: Reference torque $\boldsymbol{T}_\mathrm{ref}$ from quaternion feedback controller

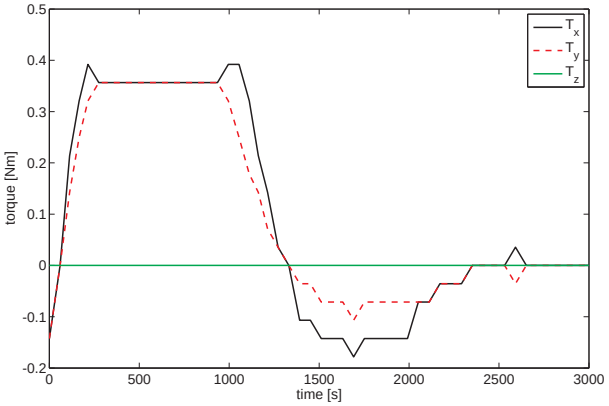

Figure 8: Achievable torque $\boldsymbol{T}_\mathrm{act}$ from RCD actuator, assuming constant pitch angle $\alpha = 0$ during the manoeuvre

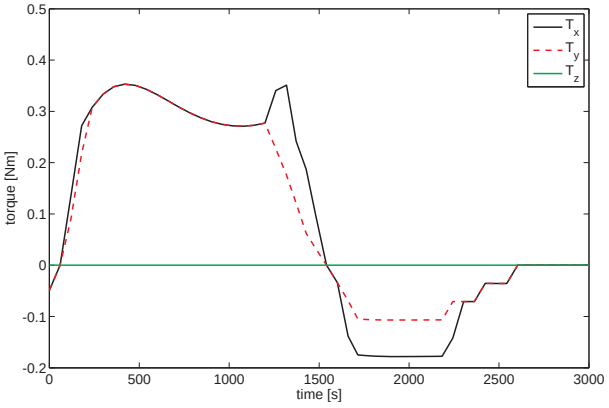

Figure 9: Achievable torque $\boldsymbol{T}_\mathrm{act}$ from RCD actuator and considering variation of SRP with surface pitch angle α

V. CONCLUSIONS

A discrete array of reflectivity control devices across the surface of a square rigid membrane spacecraft has been proposed to investigate flexible and lightweight attitude control for Gossamer spacecraft, without the use of mechanical systems or thrusters. Each cell can maintain two states, either 'on' (high reflectivity) or 'off' (low reflectivity). The achievable discrete in-plane torques have been calculated for a given membrane size, as a function of number, position and activation state of the coating elements as free parameters. The concept has been demonstrated by performing a basic Sun-pointing manoeuvre of a 100 m edge-length membrane spacecraft on a Sun-centred orbit at 1 AU solar distance. To this aim, the optical actuator model has been implemented into a quaternion feedback control scheme. Starting from an arbitrary initial attitude and angular rate, a (4,4)-array of reflectivity cells has been employed, which can obtain $65,536$ reflectivity combinations and 376 discrete torques in the membrane plane. The array was able to steer the structure into final resting attitude, despite the fact that the variation in discrete torques that can be generated are limited. Compared to the reference control torques that were computed by the quaternion feedback controller to steer the spacecraft manoeuvre ideally, the optical control-array torques have been in good agreement. However, the total manoeuvre time has been found to be twice the reference manoeuvre time, which was due to the minimum threshold of discrete torques that can be generated by the employed reflectivity array. Since the paper could demonstrate the principle use of reflectivity control devices for the control of large and ultra-lightweight Gossamer membrane spacecraft, the concept of optical attitude control may contribute to reduce the overall system mass and therefore reducing launch costs.

ACKNOWLEDGMENTS

This work was funded by the European Research Council Advanced Investigator Grant - 227571: VISIONSPACE: Orbital Dynamics at Extremes of Spacecraft Length-Scale.

REFERENCES

[1] H Demiryont and D Moorehead. Electrochromic emissivity modulator for spacecraft thermal management. *Solar Energy Materials and Solar Cells*, 93(12):2075–2078, 2009.

[2] O. Mori, Y. Tsuda, H. Sawada, R. Funase, T. Yamamoto, T. Saiki, K. Yonekura, H. Hoshino, H. Minamino, T. Endo, and J. Kawaguchi. World's first demonstration of solar power sailing by ikaros. In *Proceedings of the Second International Symposium on Solar Sailing (ISSS 2010)*, 2010.

[3] C. R. McInnes. *Solar Sailing: Technology, Dynamics and Mission Applications*, pages 1–55. Springer-Praxis Series in Space Science and Technology, Springer-Verlag, Berlin, 1999.

[4] H. Schaub. *Analytical Mechanics of Space Systems, 2nd Edition.* AIAA Educational Series, 2009.

[5] J. Kuipers. *Quaternions and Rotation Sequences.* Princeton University Press, 1999.

[6] A. Hanson. *Visualizing Quaternions.* Morgan Kaufmann, 2006.

[7] L.F. Shampine, I. Gladwell, and S. Thompson. *Solving ODEs with MATLAB*, pages 134–143. Cambridge University Press, 2003.

[8] E. Fresk and G. Nikolakopoulos. Full quaternion based attitude control for a quadrotor. In *Control Conference (ECC), 2013 European*, pages 3864–3869.

[9] David W. Sleight and Danniella M. Muheim. Parametric studies of square solar sails using finite element analysis. In *Collect. of Pap. - 45th AIAA/ASME/ASCE/AHS/ASC Struct., Struct. Dyn. and Mater. Conf.; 12th AIAA/ASME/AHS Adapt. Struct. Conf.; 6th AIAA Non-Deterministic Approaches Forum; 5th AIAA Gossamer Spacecraft Forum, April 19, 2004 - April 22, 2004*, volume 1 of *Collection of Technical Papers - AIAA/ASME/ASCE/AHS/ASC Structures, Structural Dynamics and Materials Conference*, pages 85–97. American Inst. Aeronautics and Astronautics Inc., 2004.

[10] DuPont. Kapton technical data sheet. DuPont High Performance Films, Retrieved 5 November 2013. "http://www2. dupont.com/Kapton/en_US/assets/downloads/pdf/HN_datasheet.pdf".